

Biphasic Behavior of the High-Spin \rightarrow Low-Spin Relaxation of [Fe(btpa)](PF₆)₂ in Solution (btpa = *N,N,N',N'*-Tetrakis(2-pyridylmethyl)-6,6'-bis(aminomethyl)-2,2'-bipyridine)

Sabine Schenker,^{*,†} Paul C. Stein,[†] Juliusz A. Wolny,[‡] Clare Brady,[§] John J. McGarvey,[§] Hans Toftlund,[†] and Andreas Hauser^{||}

Kemisk Institut, Syddansk Universitet, Campusvej 55, 5230 Odense M, Denmark, Wydział Chemii, Uniwersytet Wrocławski, ul. F. Joliot-Curie 14, 50383 Wrocław, Poland, School of Chemistry, Queen's University of Belfast, Stranmillis Road, Belfast BT9 5AG, Northern Ireland, and Département de chimie physique, Université de Genève, 30 quai Ernest-Ansermet, 1211 Genève 4, Switzerland

Received June 16, 2000

The light-induced high-spin \rightarrow low-spin relaxation for the Fe(II) spin-crossover compounds [Fe(btpa)](PF₆)₂ and [Fe(bbdpa)](PF₆)₂ in solution, where btpa is the potentially octadentate ligand *N,N,N',N'*-tetrakis(2-pyridylmethyl)-6,6'-bis(aminomethyl)-2,2'-bipyridine and bbdpa is the analogous hexadentate ligand *N,N'*-bis(benzyl)-*N,N'*-bis(2-pyridylmethyl)-6,6'-bis(aminomethyl)-2,2'-bipyridine, respectively, has been studied by temperature-dependent laser flash photolysis. [Fe(bbdpa)](PF₆)₂ shows single-exponential ⁵T₂ \rightarrow ¹A₁ relaxation kinetics, whereas [Fe(btpa)](PF₆)₂ exhibits solvent-independent biphasic relaxation kinetics. The fast process of [Fe(btpa)](PF₆)₂ with a rate constant, *k*_{H_L}, of 2.5 \times 10⁷ s⁻¹ at 295 K and an activation energy, *E*_a, of 1294(26) cm⁻¹ in methanol can be assigned to the ⁵T₂ \rightarrow ¹A₁ relaxation as well. The slow process with a *k*_{H_L}(295 K) of 3.7 \times 10⁵ s⁻¹ and a *E*_a of 2297(32) cm⁻¹ in methanol—which is the slowest light-induced relaxation process observed so far for an Fe(II) spin-crossover complex in solution—is assigned to a coupling of the ⁵T₂ \rightarrow ¹A₁ relaxation process to a geometrical rearrangement within the pendent pyridyl arms.

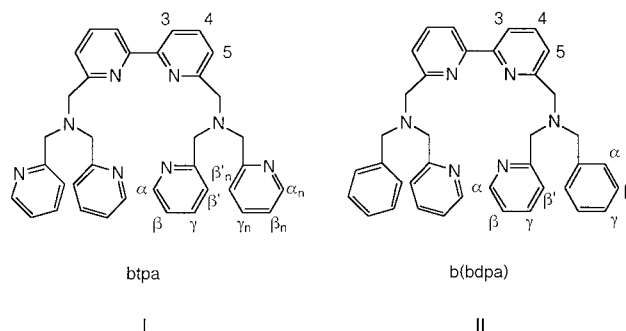
Introduction

Light-induced spin-state conversion as first observed in solution¹ and subsequently in the solid state,² is ideally suited for studying the intersystem crossing (ISC) dynamics in Fe(II) spin-crossover systems.^{3,4} The light-induced, metastable high-spin state has a lifetime of typically a few tens to hundreds of nanoseconds at ambient temperature,⁵ whereas it can live for up to several days at cryogenic temperatures.^{2,6–7} Coupling of the spin transition to structural modifications of the ligand, such as for example light-induced ligand isomerization,⁸ offers a possibility of slowing the relaxation process also at elevated temperatures.

Biphasic relaxation kinetics have been reported for [Fe(tpchxn)](ClO₄)₂ (tpchxn = tetrakis(2-pyridylmethyl)-*trans*-1,2-cyclohexanediamine) and [Fe(tp[10]aneN₃)](ClO₄)₂ (tp[10]aneN₃ = *N,N',N''*-tris(2-pyridylmethyl)-1,4,7-triazacyclodecane) in solution.^{9,10} For the former system, coupling of the high-spin \rightarrow

low-spin (HS \rightarrow LS) relaxation to a solvent-induced conformational change of the cyclohexyl ring has been postulated, whereas coupling to an isomerization within the macrocyclic moiety of the ligand has been assumed for the latter.

Here we present a study of the relaxation kinetics following the light-induced population of the HS state via the ¹A₁ \rightarrow ¹MLCT (metal-to-ligand charge transfer) excitation of [Fe(btpa)](PF₆)₂ (btpa = *N,N,N',N'*-tetrakis(2-pyridylmethyl)-6,6'-bis(aminomethyl)-2,2'-bipyridine) (**I**) in solution using a number of different solvents. Its biphasic kinetics are discussed with respect to the single-exponential kinetics of the HS \rightarrow LS relaxation as observed for the analogous [Fe(bbdpa)](PF₆)₂ (bbdpa = *N,N'*-bis(benzyl)-*N,N'*-bis(2-pyridylmethyl)-6,6'-bis(aminomethyl)-2,2'-bipyridine) (**II**) in methanol. The former



complex, consisting of a potentially octadentate ligand with a bipyridyl backbone and four pendent pyridyl arms, only two of

[†] Syddansk Universitet.
[‡] Uniwersytet Wrocławski.
[§] Queen's University of Belfast.
^{||} Université de Genève.

- (1) McGarvey, J. J.; Lawthers, I. *J. Chem. Soc., Chem. Commun.* **1982**, 906.
- (2) Decurtins, S.; Gütllich, P.; Köhler, C. P.; Spiering, H.; Hauser, A. *Chem. Phys. Lett.* **1984**, 139, 1.
- (3) Hauser, A. *Coord. Chem. Rev.* **1991**, 111, 275.
- (4) Hauser, A. *Comments Inorg. Chem.* **1995**, 17, 17.
- (5) Beattie, J. K. *Adv. Inorg. Chem.* **1988**, 32, 1.
- (6) Decurtins, S.; Gütllich, P.; Hasselbach, K. M.; Hauser, A.; Spiering, H. *Inorg. Chem.* **1985**, 24, 2174.
- (7) Hauser, A. *J. Chem. Phys.* **1991**, 94, 2741.
- (8) Boillot, M.-L.; Roux, C.; Audière, J.-P.; Dausse, A.; Zarembowitch, J. *Inorg. Chem.* **1996**, 35, 3975.
- (9) McCusker, J. K.; Toftlund, H.; Rheingold, A.; Hendrickson, D. N. *J. Am. Chem. Soc.* **1993**, 115, 1797.

- (10) Al-Obaidi, A. H. R.; McGarvey, J. J.; Taylor, K. P.; Bell, S. E. J.; Jensen, K. B.; Toftlund, H. *J. Chem. Soc., Chem. Commun.* **1993**, 536.

which are coordinated to the Fe(II) ion, exhibits spin-crossover behavior in solution. The latter complex, in which both uncoordinated pyridyl arms have been replaced by benzyl groups, is predominately in the LS state up to ambient temperature.

Experimental Section

Preparation of Compounds. Commercially available chemicals were purchased and used without further purification unless stated otherwise. Methanol was distilled from Mg prior to use. The syntheses of the Fe(II) complexes were carried out under nitrogen using standard Schlenk techniques. Elemental analyses have been performed at the microanalytical laboratory of the H. C. Ørsted Institute, Copenhagen.

btpa. The free ligand btpa was prepared as described by Døssing et al.¹¹ from bis(2-pyridylmethyl)amine and 6,6'-bis(bromomethyl)-2,2'-bipyridine.

[Fe(btpa)](PF₆)₂. FeSO₄·7H₂O (0.083 g, 0.3 mmol) was added to btpa (0.174 g, 0.3 mmol) dissolved in methanol/water (5:4) (9 mL), and the resulting mixture was stirred for 15 min. The solution turned dark red. Then, NH₄PF₆ (0.489 g, 3 mmol) was added, resulting in a dark red precipitation. The product was collected and washed with ice-cold water. Yield: 0.255 g (92%). Anal. Calcd for FeC₃₆H₃₄N₈P₂F₁₂·H₂O: C, 45.88; H, 3.85; N, 11.89. Found: C, 45.23; H, 3.79; N, 11.66. ¹H NMR (*T* = 188 K, CD₃OD, 500 MHz): δ 8.75 (d, *J* = 4.1 Hz, 2H, H_α(py_n)), 8.47 (d, *J* = 7.8 Hz, 2H, H₃(bpy)), 8.04 (t, *J* = 7.8 Hz, 2H, H_γ(py_n)), 8.03 (t, *J* = 8.0 Hz, 2H, H₄(bpy)), 7.91 (d, *J* = 7.5 Hz, 2H, H_β(py_n)), 7.78 (t, *J* = 7.4 Hz, 2H, H_γ(py_c)), 7.58 (t, *J* = 6.1 Hz, 2H, H_β(py_n)), 7.54 (d, *J* = 7.9 Hz, 2H, H_β(py_c)), 7.53 (d, *J* = 7.6 Hz, 2H, H₅(bpy)), 7.13 (t, *J* = 6.8 Hz, 2H, H_β(py_c)), 7.03 (d, *J* = 4.4 Hz, 2H, H_α(py_c)), 5.12 (dd, *J* = 16 Hz, 432 Hz, 4H, CH₂), 4.87 (dd, *J* = 17 Hz, 442 Hz, 4H, CH₂), 4.19 (dd, *J* = 12 Hz, 606 Hz, 4H, CH₂).

b(bdpa). The free ligand b(bdpa) was prepared analogously to the procedure for btpa,¹¹ using (*N,N*-benzyl-2-pyridylmethyl)amine instead of bis(2-pyridylmethyl)amine. It was obtained as a yellow-brown oil. Yield: 1.5 g (88%).

(*N,N*-Benzyl-2-pyridylmethyl)amine. 2-Pyridinecarbaldehyde (4 g, 37.3 mmol) and benzylamine (4 g, 37.3 mmol) were dissolved in absolute ethanol (100 mL) and boiled for 2 h. The solvent was removed and the residue dissolved in methanol (50 mL). NaBH₄ (0.76 g, 20.1 mmol) was added in small portions and stirred overnight. The solvent was removed, and the residue was dissolved in methylenechloride, dried over MgSO₄ and filtered. Vacuum distillation yielded 2 g (27%) of liquid (*N,N*-benzyl-2-pyridylmethyl)amine.

[Fe(b(bdpa))](PF₆)₂. FeSO₄·7H₂O (0.070 g, 0.25 mmol) in water (5 mL) was added to b(bdpa) (0.144 g, 0.25 mmol) dissolved in methanol (15 mL). The solution was stirred for 15 min and turned deep red. Additional water (10 mL) and NH₄PF₆ (0.750 g, 4.6 mmol) were added, causing a dark red precipitation immediately. The product was filtrated and washed with water and diethyl ether. Yield: 0.19 g (82%). Anal. Calcd for FeC₃₈H₃₆N₆P₂F₁₂·H₂O: C, 48.56; H, 4.07; N, 8.93. Found: C, 48.23; H, 3.90; N, 8.86. ¹H NMR (*T* = 223 K, CD₃OD, 500 MHz): δ 8.52 (br s, 2H, H₃(bpy)), 8.05 (t, 2H, H₄(bpy)), 7.83 (t, 2H, H_γ(py)), 7.73 (d, 4H, H_α(bz)), 7.65 (br s, 2H, H₅(bpy)), 7.61 (br s, 2H, H_β(py)), 7.56 (t, 6H, H_β(bz)), 7.22 (br s, 2H, H_β(py)), 7.18 (br s, 2H, H_α(py)), 5.19 (d, 4H, CH₂), 4.78 (d, 4H, CH₂), 4.12 (d, 4H, CH₂).

Physical Measurements. ¹H NMR spectra were recorded on a Varian Unity 500 spectrometer in CD₃OD and referenced to tetramethylsilane. Laser flash photolysis experiments were performed using the pump-probe technique as described in refs 12 and 13. Pulsed excitation at 532 nm (SH of a Quantel Brilliant or a Quanta-Ray DCR2 Nd:YAG laser) led to an efficient population of the HS state, manifesting itself in a bleaching of the characteristic CT band of the LS species (see below). The recovery of the transient bleaching was

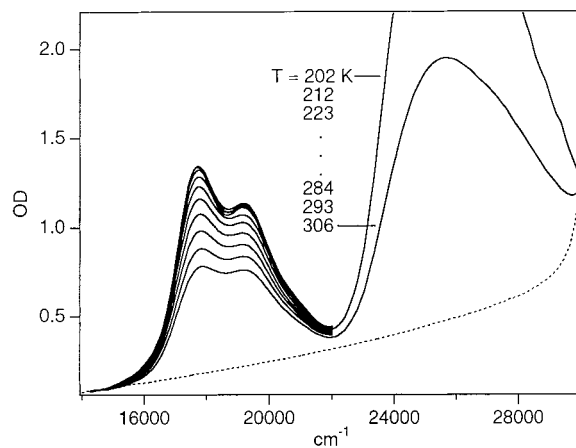


Figure 1. Absorption spectra of [Fe(btpa)](PF₆)₂ (—) between 306 and 202 K and [Zn(btpa)](PF₆)₂ (---) at ambient temperature in methanol (*c* = 10⁻³ M, path length *d* = 0.1 cm).

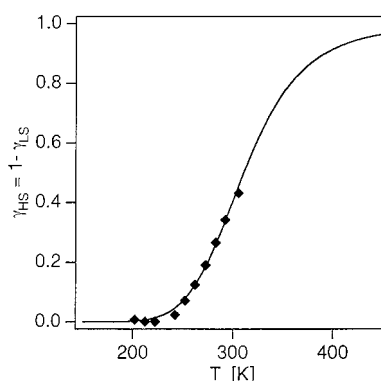


Figure 2. Temperature dependence of the HS fraction, $\gamma_{\text{HS}} = 1 - \gamma_{\text{LS}}$, for [Fe(btpa)](PF₆)₂ in methanol (◆) and the corresponding least-squares fit (—) with $\Delta H_{\text{HL}}^{\circ} = 2303(87) \text{ cm}^{-1}$ and $\Delta S_{\text{HL}}^{\circ} = 7.4(3) \text{ cm}^{-1}/\text{K}$.

monitored with a collinear probe beam from a 100 W tungsten lamp at different wavelengths. Sample temperatures down to 170 K were achieved using a closed cycle refrigerator (Oxford Instruments CCC1204).

Results

Figure 1 shows the temperature-dependent absorption spectra of [Fe(btpa)](PF₆)₂ in methanol (*c* = 10⁻³ M, path length *d* = 0.1 cm) between 202 and 306 K. They are corrected for solvent contraction of ~20% between 306 and 202 K.¹⁴ The absorption band in the visible region, with maxima at 17 700 and 19 200 cm⁻¹, which increases in intensity with decreasing temperatures, is due to MLCT transitions of the LS species. From the fact that, below ~230 K, the intensity of this band no longer increases, it can be inferred that the complexes are completely in the LS state below this temperature. The intensity of the MLCT transition for Fe(II) polypyridyl complexes in the HS state are generally more than 1 order of magnitude smaller than those for complexes in the LS state. Assuming the hypothetical absorption spectrum of the HS species to be similar to the absorption spectrum of the analogous [Zn(btpa)](PF₆)₂ compound in methanol (see Figure 1) allows the LS fraction as a function of temperature, $\gamma_{\text{LS}}(T)$, to be extracted from the integrated absorption bands. In Figure 2 the resulting transition curve for the thermal LS ⇌ HS equilibrium, plotted as $\gamma_{\text{HS}}(T) = 1 - \gamma_{\text{LS}}(T)$, is given. Below 230 K $\gamma_{\text{HS}} = 0$, and it reaches a value of ~0.45 at 306 K. From a least-squares fit, using the

(11) Døssing, A.; Hazell, A.; Toftlund, H. *Acta Chem. Scand.* **1996**, *50*, 95.

(12) Hauser, A.; Vef, A.; Adler, P. *J. Chem. Phys.* **1991**, *95*, 8410 and references therein.

(13) McGarvey, J. J.; Lawthers, I.; Heremans, K.; Toftlund, H. *Inorg. Chem.* **1990**, *29*, 252.

(14) *Landolt-Börnstein*; Springer-Verlag: Berlin, **1971**; Vol. II(1), p 662.

Table 1. Thermodynamic Parameters $\Delta H_{\text{HL}}^\circ$ and $\Delta S_{\text{HL}}^\circ$ of the Thermal Spin Equilibrium of $[\text{Fe}(\text{btpa})](\text{PF}_6)_2$, Activation Energies, E_a , and Rate Constants, $k_{\text{HL}}(295 \text{ K})$, for the $\text{HS} \rightarrow \text{LS}$ Relaxation of $[\text{Fe}(\text{btpa})](\text{PF}_6)_2$ and $[\text{Fe}(\text{b(dpa)})](\text{PF}_6)_2$ in Methanol

	$[\text{Fe}(\text{btpa})](\text{PF}_6)_2$	$[\text{Fe}(\text{b(dpa)})](\text{PF}_6)_2$
$\Delta H_{\text{HL}}^\circ$ (cm^{-1})	2303(87)	
$\Delta S_{\text{HL}}^\circ$ (cm^{-1}/K)	7.4(3)	
E_a^{fast} (cm^{-1})	1294(26)	1207(10)
$k_{\text{HL}}^{\text{fast}}(295 \text{ K})$ (s^{-1})	2.5×10^7	6.7×10^6 ^a
E_a^{slow} (cm^{-1})	2297(32)	
$k_{\text{HL}}^{\text{slow}}(295 \text{ K})$ (s^{-1})	3.7×10^5	

^a At 273 K.

equation for the Gibbs free energy of a diluted system, $\Delta G_{\text{HL}}^\circ = \Delta H_{\text{HL}}^\circ - T\Delta S_{\text{HL}}^\circ = -k_{\text{B}}T \ln[\gamma_{\text{HS}}/\gamma_{\text{LS}}]$, values for the thermodynamic parameters $\Delta H_{\text{HL}}^\circ$ and $\Delta S_{\text{HL}}^\circ$ of 2303(87) cm^{-1} and 7.4(3) cm^{-1}/K , respectively, were obtained. They were regarded as temperature independent within the temperature interval of the spin transition.

Temperature-dependent ^1H NMR spectra of $[\text{Fe}(\text{btpa})](\text{PF}_6)_2$ and $[\text{Fe}(\text{b(dpa)})](\text{PF}_6)_2$ in CD_3OD have been recorded to obtain some structural information as well as additional information on the thermal $\text{LS} \rightleftharpoons \text{HS}$ equilibrium. The ^1H resonances for $[\text{Fe}(\text{btpa})](\text{PF}_6)_2$ and $[\text{Fe}(\text{b(dpa)})](\text{PF}_6)_2$ at 188 and 223 K, respectively, are summarized in Table 2. Both spectra display three sets of signals in the regions between 8.8 and 7.0 ppm and between 5.6 and 3.6 ppm. On the basis of the 2D COSY spectrum and by comparison with the spectrum of $[\text{Fe}(\text{b(dpa)})](\text{PF}_6)_2$, the signals in the former region can be assigned unambiguously to the bipyridine and to two different pyridine moieties of the $[\text{Fe}(\text{btpa})](\text{PF}_6)_2$ complex, reflecting that only two of the four pendent pyridyl arms are coordinated, whereas the signals in the latter region are due to three inequivalent methylene groups of the complex. This spectrum clearly shows that the complexes are completely diamagnetic at 188 K and have C_2 symmetry. At $\sim 230 \text{ K}$ the resonances in the pyridine and methylene regions collapse, and with increasing temperatures relatively large paramagnetic shifts of the resonances, up to 45 ppm at 328 K, are observed. These findings confirm that the $[\text{Fe}(\text{btpa})](\text{PF}_6)_2$ complexes are completely in the LS state below $\sim 230 \text{ K}$ (see Figure 2), as extracted from the temperature-dependent absorption spectra in Figure 1.

The kinetics of the $\text{HS} \rightarrow \text{LS}$ relaxation of $[\text{Fe}(\text{btpa})](\text{PF}_6)_2$ and $[\text{Fe}(\text{b(dpa)})](\text{PF}_6)_2$ in methanol were determined by monitoring the transient bleaching of the $^1\text{A}_1 \rightarrow ^1\text{MLCT}$ absorption band. Representative relaxation curves are shown in Figure 3. Biphasic relaxation behavior was observed for the former, whereas the latter exhibits single-exponential behavior. In Figure 4a the relaxation rate constants for the various processes, as obtained from biexponential and single-exponential least-squares fits, respectively, are plotted vs $1/T$ (Arrhenius plot). At ambient temperature, the ratio of the rate constants of the fast and the slow processes in $[\text{Fe}(\text{btpa})](\text{PF}_6)_2$ is approximately 70, and it increases to 3 orders of magnitude at 190 K. The rate constants of the fast process in $[\text{Fe}(\text{btpa})](\text{PF}_6)_2$ and the single process in the $[\text{Fe}(\text{b(dpa)})](\text{PF}_6)_2$ system are comparable, with values of about $1 \times 10^7 \text{ s}^{-1}$ at ambient temperature. This value falls well within the range of 10^6 – 10^8 s^{-1} , typically found for Fe(II) spin-crossover and Fe(II) LS compounds close to the crossover point.^{5,15} The corresponding activation energies as obtained from a linear least-squares fit to the Arrhenius plots of Figure 4a are 1294(26) and 1207(10) cm^{-1} , respectively.

For $[\text{Fe}(\text{btpa})](\text{PF}_6)_2$, the activation energy of the slow process is 2297(32) cm^{-1} . This is approximately twice the value of the fast process. For this compound, the biphasic relaxation behavior has been observed not only in methanol but also in acetonitrile and aceto/butyronitrile (4:5). The Arrhenius plots in Figure 4b present a comparison of the relaxation rate constants, k_{obs} , in all three solvents. Within experimental error they are the same in all three solvents.

The amplitudes of the transient signals of $[\text{Fe}(\text{btpa})](\text{PF}_6)_2$ in solution do vary relative to each other with temperature for the slow and the fast relaxation processes (see Figure 3a). Figure 5a shows the ratio of the amplitudes, $A_{\text{fast}}/A_{\text{slow}}$, for $[\text{Fe}(\text{btpa})](\text{PF}_6)_2$ in methanol. At ambient temperature, the $\text{HS} \rightarrow \text{LS}$ relaxation is dominated by the slow process, whereas with decreasing temperature the fast process becomes the dominant one. Below 200 K the slow relaxation process has almost disappeared. In Figure 5a the viscosity of methanol, η , as a function of temperature is included.¹⁶ Both curves indicate the same temperature dependence. In fact, as can be seen from Figure 5b there is a linear correlation between the ratio $A_{\text{fast}}/A_{\text{slow}}$ and η . Therefore, the formation of the transient state, from which the subsequent slow back-relaxation to the LS state is observed, is related to the rigidity of the solvent surrounding the complex.

To obtain further information regarding the transient states involved in the biphasic relaxation kinetics of $[\text{Fe}(\text{btpa})](\text{PF}_6)_2$ in methanol, excited-state difference absorption spectra were recorded. Figure 6 shows the spectra at 296 K for the slow process and at 203 K for the fast process, that is, the dominant process at the respective temperature. The missing part in the spectra between 18 520 and 19 230 cm^{-1} is due to the notch filter used for blocking the excitation beam. Within experimental accuracy, there is no difference observable in the two spectra. Both indicate a bleaching of the two LS MLCT bands with maxima at about 17 700 and 25 500 cm^{-1} in agreement with the absorption spectra in Figure 1.

Discussion

Biphasic kinetics for the light-induced $\text{HS} \rightarrow \text{LS}$ relaxation have been observed previously in other systems, for instance, for $[\text{Fe}(\text{tpchxn})](\text{ClO}_4)_2$ in methanol,⁹ and for $[\text{Fe}(\text{tp}[10]\text{aneN}_3)](\text{ClO}_4)_2$ in aceto- and propionitrile.^{10,17} McCusker et al. associate the biphasic behavior of the former to two different solvent-induced conformations of the cyclohexyl ring in the HS state, but surprisingly, this phenomenon has been observed in methanol only, whereas single-exponential relaxation kinetics have been found in acetonitrile and DMF.¹³ The biphasic behavior of the latter was assigned to a coupling of the $\text{HS} \rightarrow \text{LS}$ relaxation to the isomerization of the aliphatic ring of the macrocyclic ligand.

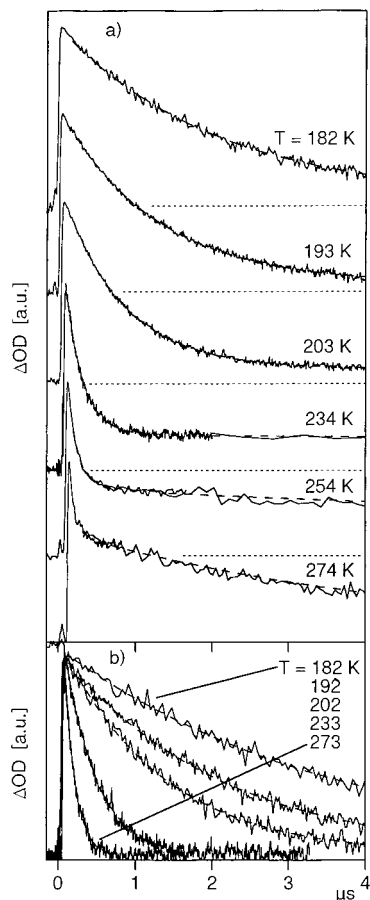
The observation that $[\text{Fe}(\text{btpa})](\text{PF}_6)_2$ exhibits biphasic light-induced relaxation in solution, whereas the relaxation rates of the analogous $[\text{Fe}(\text{b(dpa)})](\text{PF}_6)_2$, where the two noncoordinating pyridyl groups are replaced by benzyl groups, are single-exponential, shows that the biphasic behavior is due to the potentially octadentate nature of btpa. As mentioned above, the fast process in $[\text{Fe}(\text{btpa})](\text{PF}_6)_2$ is comparable to the $\text{HS} \rightarrow \text{LS}$

(15) König, E. *Struct. Bonding (Berlin)* **1991**, 76, 51.(16) *Handbook of Chemistry and Physics*; CRC Press Inc.: Boca Raton, FL, 1991.

(17) Jensen, K. B. Ph.D. Thesis, Odense Universitet, Odense, Denmark, 1997; see also references therein.

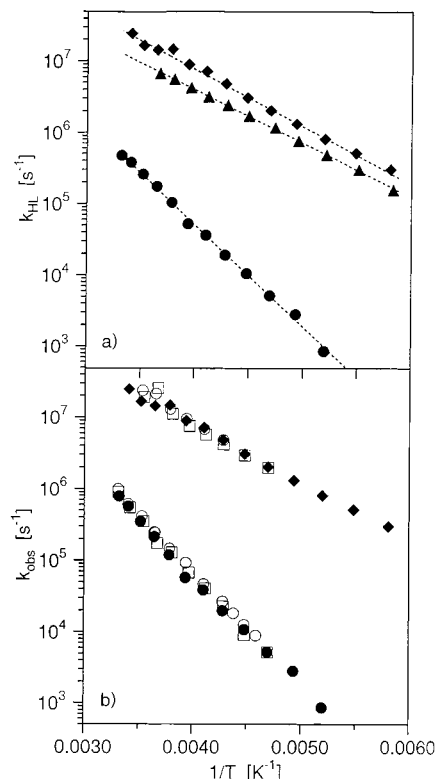
Table 2. ^1H NMR Chemical Shifts of $[\text{Fe}(\text{btpa})](\text{PF}_6)_2$ at 188 K and $[\text{Fe}(\text{b}(\text{bdpa}))](\text{PF}_6)_2$ at 223 K in CD_3OD

	$[\text{Fe}(\text{btpa})](\text{PF}_6)_2$	$[\text{Fe}(\text{b}(\text{bdpa}))](\text{PF}_6)_2$		$[\text{Fe}(\text{btpa})](\text{PF}_6)_2$	$[\text{Fe}(\text{b}(\text{bdpa}))](\text{PF}_6)_2$
bpy 3	8.47	8.52	py γ_n	8.04	
bpy 4	8.03	8.05	py β_n'	7.91	
bpy 5	7.53	7.65	bz α		7.73
py α	7.03	7.18	bz β		7.56
py β	7.13	7.22	bz γ		7.56
py γ	7.78	7.83	CH_2	5.12	5.19
py β	7.54	7.61	CH_2	4.87	4.78
py α_n	8.75		CH_2	4.19	4.12
py β_n	7.58				

**Figure 3.** HS \rightarrow LS relaxation curves (—) and the corresponding least-squares fits (---) of (a) the biphasic process of $[\text{Fe}(\text{btpa})](\text{PF}_6)_2$ in methanol detected at 570 nm and (b) the single process of $[\text{Fe}(\text{b}(\text{bdpa}))](\text{PF}_6)_2$ in methanol detected at 500 nm after pulsed laser excitation at 532 nm in the temperature range between 182 and 274 K.

relaxation of $[\text{Fe}(\text{b}(\text{bdpa}))](\text{PF}_6)_2$. The corresponding values for the relaxation rate constants, $k_{\text{HL}}^{\text{fast}}$, at ambient temperature of 10^7 s^{-1} and the activation energies, E_a^{fast} , of $\sim 1200 \text{ cm}^{-1}$, agree well with the respective ranges of 10^6 – 10^8 s^{-1} and 800 – 1500 cm^{-1} typically found for Fe(II) spin-crossover and LS compounds close to the spin-crossover point, in solution.^{4,5} Therefore, the fast relaxation process can be assigned to the direct $^5\text{T}_2 \rightarrow ^1\text{A}_1$ relaxation for both compounds, involving basically the metal–ligand bond length as reaction coordinate.

The slow process of $[\text{Fe}(\text{btpa})](\text{PF}_6)_2$, with a $k_{\text{HL}}^{\text{slow}}$ of $3.7 \times 10^5 \text{ s}^{-1}$ at 295 K in methanol is the slowest light-incurred relaxation process observed so far for an Fe(II) spin-crossover complex in solution. The value for E_a^{slow} of $2297(32) \text{ cm}^{-1}$ is almost twice as large as that of the fast process. Such a large value indicates that a larger geometrical rearrangement of the coordination sphere takes place than simple lengthening of the metal–ligand bonds as commonly observed for spin-crossover

**Figure 4.** (a) Logarithmic plot of k_{HL} vs $1/T$ for the HS \rightarrow LS relaxation of $[\text{Fe}(\text{btpa})](\text{PF}_6)_2$ [\blacklozenge] fast process, [\bullet] slow process] and $[\text{Fe}(\text{b}(\text{bdpa}))](\text{PF}_6)_2$ [\blacktriangle] in methanol. The broken lines represent the classical Arrhenius behavior with activation energies, E_a , of $2297(32)$ and $1294(26) \text{ cm}^{-1}$ for the slow and fast relaxation processes, respectively, for $[\text{Fe}(\text{btpa})](\text{PF}_6)_2$ and of $1207(10) \text{ cm}^{-1}$ for $[\text{Fe}(\text{b}(\text{bdpa}))](\text{PF}_6)_2$. (b) Logarithmic plot of the relaxation rate constants, k_{obs} , vs $1/T$ for $[\text{Fe}(\text{btpa})](\text{PF}_6)_2$ in methanol (\blacklozenge , \bullet), acetonitrile (\odot), and aceto/butyronitrile (4:5) (\square).

systems. Solvent reorganization plays a minor role as long as there is no direct coordination of the solvent, and according to Buhks et al.¹⁸ can generally be disregarded. Such is the case for $[\text{Fe}(\text{btpa})](\text{PF}_6)_2$, in agreement with the observation that solvent variation has no influence on the rate constants of the biphasic relaxation (see Figure 4b). The large value for E_a^{slow} must therefore be due to intrinsic properties of the complex.

From crystal structure analysis of $[\text{Fe}(\text{btpa})](\text{PF}_6)_2$ it is known that the Fe(II) complexes occupy two crystallographically nonequivalent lattice sites.¹⁹ One site has an almost octahedral $[\text{FeN}_6]$ coordination sphere with mean Fe–N bond lengths of 2.00 \AA ($r_{\text{Fe-N}_{\text{amine}}} = 1.94 \text{ \AA}$ and $r_{\text{Fe-N}_{\text{pyridine}}} = 2.11 \text{ \AA}$). The other site consists of a highly distorted $[\text{FeN}_6]$ unit with mean Fe–N bond lengths of 2.23 \AA ($r_{\text{Fe-N}_{\text{amine}}} = 2.18 \text{ \AA}$ and $r_{\text{Fe-N}_{\text{pyridine}}} =$

(18) Buhks, E.; Navon, G.; Bixon, M.; Jortner, J. *J. Am. Chem. Soc.* **1980**, *102*, 2918.

(19) Wolny, J.; Toftlund, H.; Hazell, A. Unpublished results.

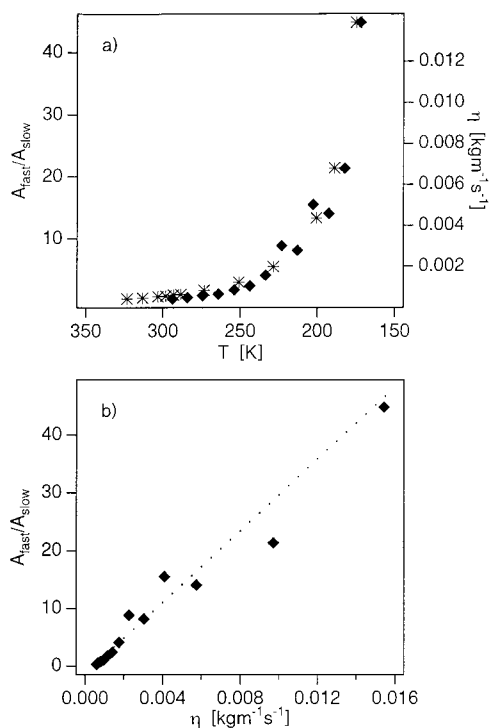


Figure 5. (a) Comparison of A_{fast}/A_{slow} (◆) for $[\text{Fe}(\text{btpa})](\text{PF}_6)_2$ in methanol with the viscosity, η , of methanol (*)¹⁴ as a function of temperature. A_{fast} and A_{slow} are the amplitudes of the transient bleached LS signal of the fast and slow relaxation processes, respectively. (b) A_{fast}/A_{slow} (◆) vs η .

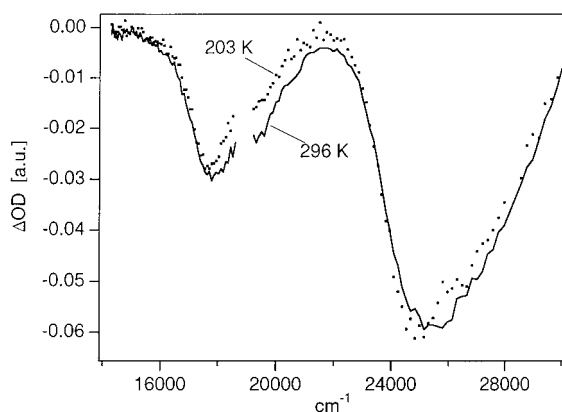


Figure 6. Excited-state difference absorption spectra of $[\text{Fe}(\text{btpa})](\text{PF}_6)_2$ in methanol at 296 and 203 K of the slow (—) and fast (small solid squares) relaxation processes, respectively.

2.34 Å) and a twisting of the bipyridyl ligand backbone along the 2,2'-C,C bond. One of the two noncoordinating pyridyl arms is pointing toward the Fe center with an Fe–N distance of only 3.16 Å. The former site can be assigned to a LS state and the latter to a HS state, in agreement with the solid-state Mössbauer spectra, which show two doublets at $\delta_{HS} = 1.04$ mm/s ($\Delta E_Q^{HS} = 2.87$ mm/s) and $\delta_{LS} = 0.39$ mm/s ($\Delta E_Q^{LS} = 0.38$ mm/s). The relative intensity of the signals is the same at both ambient and liquid nitrogen temperatures. $[\text{Fe}(\text{btpa})](\text{PF}_6)_2$ in the solid state does not exhibit a thermal spin transition. This indicates that for $[\text{Fe}(\text{btpa})]^{2+}$ there is a low-lying HS state with a very distorted geometry, and that in the solid state packing forces may actually lock it in this state. On the basis of the foregoing considerations, rearrangement of the chelating, potentially octadentate ligand seems to be very likely for the species in the light-induced HS state with slow relaxation in solution.

However, in this case twisting of the bipyridyl backbone can be ruled out as the crucial step, since its substitution by the planar phenanthroline has no effect on the kinetics. In fact, $[\text{Fe}(\text{b}(\text{dpa})\text{p})](\text{PF}_6)_2$ ($\text{b}(\text{dpa})\text{p} = N,N,N',N'$ -tetrakis(2-pyridylmethyl)-2,9-bis(aminomethyl)-1,10-phenanthroline) in methanol shows biphasic kinetics as well, with relaxation rate constants on the same order of magnitude.²⁰ In addition, the observation that the slow relaxation process diminishes, relative to the fast process, and finally disappears with increasing viscosity of the solvent indicates a rearrangement of the pendent pyridyl arms during the process. Since the solvation sphere of the complex turns more and more rigid with increasing bulk viscosity, the rearrangement within the pyridyl moieties becomes more and more hindered and finally stops completely.

In conclusion, for $[\text{Fe}(\text{btpa})](\text{PF}_6)_2$ in solution there are two metastable HS states with distinctly different equilibrium geometries and lifetimes. One, henceforth denoted HS_A , differs from the LS state basically by the substantially longer Fe–L bond lengths. For the other one, denoted HS_B , an additional rearrangement of the pyridyl arms is involved. The first question to consider is which one of the two HS states, HS_A or HS_B , lies lower in energy, and thus, is the thermally populated HS state of the $\text{LS} \rightleftharpoons \text{HS}$ equilibrium of $[\text{Fe}(\text{btpa})](\text{PF}_6)_2$ in solution. It was not possible to probe the involved HS state of the thermal spin transition directly, neither by temperature-dependent absorption spectroscopy nor by ¹H NMR spectroscopy. But, on the basis that the relaxation process from the HS_B state is a factor of ~ 70 slower than that from the HS_A state at ambient temperature, and that its activation energy is almost twice as large (see Figure 4a and Table 1), the HS_B state can be inferred to be at lower energy. The rearrangement within the pendent pyridyl moieties of the complex results in a less constrained state than lengthening of the metal–ligand bonds only. These considerations are confirmed by the behavior of the analogous $[\text{Fe}(\text{b}(\text{bdpa}))](\text{PF}_6)_2$. With both noncoordinating pyridyl groups replaced by benzyl rings, the $\text{HS} \rightarrow \text{LS}$ relaxation is single exponential with rate constants on the same order of magnitude as those of the fast process in $[\text{Fe}(\text{btpa})](\text{PF}_6)_2$, and the complexes are predominately in the LS state up to ambient temperature.

This is summarized in the two-dimensional configurational coordinate diagram depicted in Figure 7. The reaction coordinate of the fast process is well described by the Fe–L breathing mode, $Q_{\text{Fe-L}}$, whereas the reaction coordinate of the slow process is a combination of $Q_{\text{Fe-L}}$ and the rearrangement of the pyridyl arms, Q_{rear} . The difference between the HS_A and the LS potential wells corresponds to the difference in equilibrium configurations between the HS and the LS states, $\Delta Q_{\text{HL}} = (\sqrt{6})\Delta r_{\text{HL}}$ ($\Delta r_{\text{HL}} \approx 0.2 \text{ \AA}^{22-25}$), typically observed for Fe(II) spin-crossover and LS compounds close to the crossover point. The HS_B potential well is additionally displaced along Q_{rear} , resulting in an increase of both barrier height and thickness.

As indicated by the excited-state difference absorption spectra in Figure 6, the relaxation from both light-induced HS states, HS_A and HS_B , to the same, initial LS state takes place. But

- (20) Schenker, S.; Døssing, A. Unpublished results.
 (21) McCusker, J. K.; Walda, K. N.; Dunn, R. C.; Simon, J. D.; Magde, D.; Hendrickson, D. N. *J. Am. Chem. Soc.* **1993**, *115*, 298.
 (22) Hoselton, M. A.; Wilson, L. J.; Drago, R. S. *J. Am. Chem. Soc.* **1975**, *97*, 1722.
 (23) Mikami-Kido, M.; Konno, M.; Saito, Y. *Acta Crystallogr., Sect. B* **1982**, *36*, 275.
 (24) Wiehl, L.; Kiel, G.; Köhler, C. P.; Spiering, H.; Gütllich, P. *Inorg. Chem.* **1986**, *25*, 1565.
 (25) Letard, J.-F.; Guionneau, P.; Codjovi, E.; Lavastre, O.; Bravic, G.; Chasseau, D.; Kahn, O. *J. Am. Chem. Soc.* **1997**, *119*, 10861.

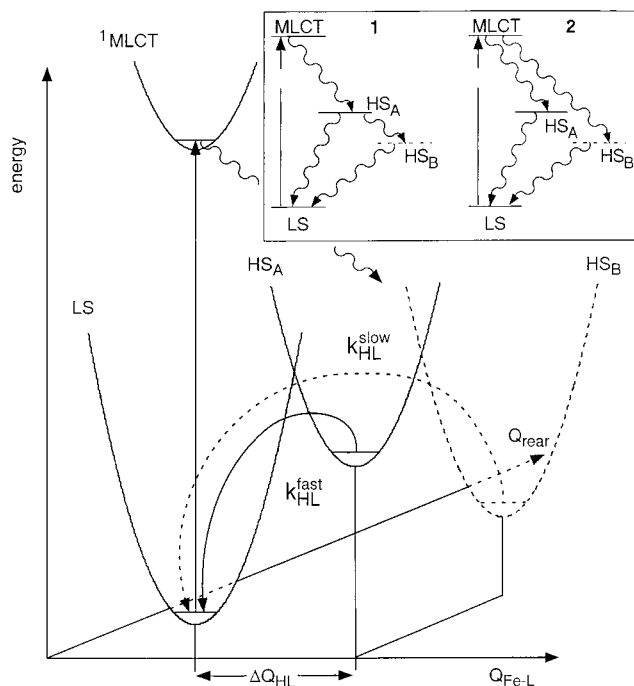


Figure 7. Configurational coordinate diagram, with the LS, MLCT, HS_A , and HS_B potential wells, schematically illustrating the biphasic $\text{HS} \rightarrow \text{LS}$ relaxation process following pulsed laser excitation into the ${}^1\text{A}_1 \rightarrow {}^1\text{MLCT}$ transition of $[\text{Fe}(\text{btpa})](\text{PF}_6)_2$ in solution. Inset: Scheme, showing the two possible pathways, mechanism 1 and 2, for the transient population of the two metastable HS_A and HS_B states and their subsequent back-relaxation to the LS state.

there are two possible pathways resulting in transient populations of the two HS states after pulsed laser excitation into the ${}^1\text{A}_1$

$\rightarrow {}^1\text{MLCT}$ transition, as sketched in the inset of Figure 7. In mechanism 1, the initially excited ${}^1\text{MLCT}$ state decays by fast ISC steps to the HS_A state, from which both direct relaxation to the LS state and relaxation to the HS_B state occur, the sum of the two rate constants being equal to the observed rate constant of the fast process. In mechanism 2, on the other hand, irradiation into the ${}^1\text{MLCT}$ state is followed by fast ISC steps into the HS_A state as well as into the HS_B state, both finally relaxing to the LS state. The two pathways cannot be distinguished on the basis of the laser flash photolysis experiments alone. These allow an indirect study of the two transient HS states only, since neither state absorbs in the visible range. McCusker et al.²¹ have shown for iron(II) polypyridyl spin-crossover as well as for LS compounds that the relaxation from the excited ${}^1\text{MLCT}$ state into the ${}^5\text{T}_2$ state takes place within a few picoseconds. On the basis of these findings, it could be argued that a larger geometrical rearrangement than lengthening of the metal–ligand bond lengths, such as rearrangement within the pendent pyridyl moieties of $[\text{Fe}(\text{btpa})](\text{PF}_6)_2$, is not probable within a few picoseconds. Therefore, it may be concluded that the consecutive decay pathway, mechanism 1, is more likely for the light-induced, biphasic $\text{HS} \rightarrow \text{LS}$ relaxation of $[\text{Fe}(\text{btpa})](\text{PF}_6)_2$ in solution.

Acknowledgment. This work was financially supported by the European Union within a TMR network (ERB-FMRX-CT98-0199) and the Swiss National Science Foundation. S.Sch. thanks the Swiss National Science Foundation for a postdoctoral grant as well and C.B. the Department of Education (Northern Ireland) for a postgraduate studentship.

IC000656T